Smith

NASA TECHNICAL TRANSLATION NASA TT F 15,233

REPRESENTATION OF HOT JET TURBULENCE BY MEANS OF ITS INFRARED EMISSION

J-F de Belleval and M. Pérulli

Translation of: "Représentation de la turbulence d'un jet chaud a partir de son émission infrarouge", Office National d'Etudes et de Recherches Aérospatiales, Châtillon, France, Report T.P. No. 1277, September 17-21, 1973, 10 pages.

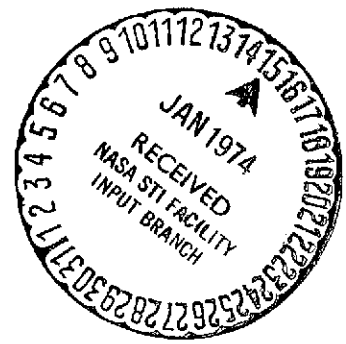

NATIONAL AERONAUTICS AND SPACE ADMINISTRATION
WASHINGTON, D. C. 20546 DECEMBER 1973

NOTATION

$C(\vec{y},\vec{\rho},\tau)$	Autocorrelation coefficient
$\vec{y}, \vec{y}', \vec{y}''$	Variable point of the source volume
ξ	Axial separation of the radiometers
τ	Time
V_c	Convection rate
$C_{12}(\xi,\tau)$	Intercorrelation coefficient
X	Jet axis
D	Diameter of the nozzle in the outlet plane
τ_m	Abscissa of the maximum of the correlation coefficient.
$\mathcal{T}$	Integral scale of lifetime
$\mathcal{L}_x$	Integral scale of length along the jet axis
ρ	Volume mass
t	Time
$\vec{v}$	Velocity of liquid
p	Pressure
$\vec{\vec{\Pi}}$	Unit tensor
$\vec{x}$	Observation point
$\hat{t}$	Delayed time (emission time)
$\mathcal{P}(\vec{x},\tau)$	Autocorrelation of the four sound fields
$\mathcal{P}(\vec{x},\omega)$	Fourier transform of $\mathcal{P}(\vec{x},\tau)$
$I(\vec{x},\omega)$	Spectral density of the far sound field
$I(\vec{x})$	Sound intensity
Θ	Angle between the jet axis and the observation point
c_o	Sound velocity in the medium at rest
V_j	Local jet velocity

REPRESENTATION OF HOT JET TURBULENCE BY MEANS OF ITS INFRARED EMISSION *

Jean-Francois de Belleval and Mariano Perulli **

1. INTRODUCTION

/ 6.2 ***

The purpose of the work carried out by the ONERA [1] in cooperation with the SNECMA [2] under the ageis of the Technical Aeronautic Service is to define a procedure for characterizing noise sources in a hot jet. The requirement for such a procedure appeared because certain limits were reached regarding noise reduction. In effect, according to work by Lighthill [3] Ribner [4] and FFOWCS-WILLIAMS [5], for moderate subsonic cold jets, there is a correspondence between theoretical models and sound measurements in the far field. These theoretical models allow the prediction of the sound field (directivity and spectrum) using turbulence variables defined with the scale of the jet volume. Nevertheless, this correspondence only applies if empirical constants are introduced and if it is assumed that the turbulence variables vary according to laws derived from the models themselves. Experimental results are also taken into account [6].

---

* National Aerospace Study and Research Office, 92320 Châtillon, France. Paper presented at the Fluid Dynamic Specialists Group of the AGARD on noise mechanisms (Memoir No. 6) Bruselles, September 17-21, 1973. TP No. 1277 (1973)

** National Aerospace Study and Research Office, 92320 Châtillon, France.

*** Numbers in the margin indicate pagination of original foreign text.

Because of this, it became necessary to characterize noise sources with a finer scale, for example, by studying the contribution of various sections of the jet,

- either by including only certain parts of the jet in the acoustical measurements (using directional microphone systems or only introducing a part of the volume source in the acoustic space [72]),

- or by adapting the image source method by making correlations between microphones located along a completely reflecting wall [8].

In addition, in order to obtain a finer spatial scale, acoustic investigators have used the following in order to characterize the turbulence of cold jets: hot wires [9, 10], acoustic receivers [11], laser strioscopy [12, 13], infrared absorption measurements [14,15] and for hot jets, infrared emission [16, 17]. Only cold jets have been subjected to acoustical investigations, performed with correlations between hot wire and microphone measurements [10, 11, 18, 19].

2. DEFINITION OF THE PROCEDURE

In the case of high or low velocity cold jets, the theoretical treatment is very complex because of the mixture of effects related to the density gradient, the temperature field and the velocity field. These effects were experimentally established [20]. A detailed theoretical analysis of these effects and a classification procedure is in progress or planned for various noise generators [21, 22].

The method of operation proposed by ONERA is a global method. Essentially, it attempts to give a qualitative evaluation of the effects of the mechanical or aerodynamic silencers on the acoustic radiation (directivity and spectrum in the far field). In this method, the jet volume is assimilated into a volume with acoustic radiation, which is everywhere characterized by space-time variables.

It is assumed:

2.1. - that the information sampling in the jet results in local information on noise sources or on their acoustic emissions,

2.2. - that from this sampling one can derive the growth in space of the turbulence variables by means of a hybrid processing of the signal,

2.3. - finally, that one can derive the acoustic radiation in the far field by applying a numerical calculation to these variables. For this, the inhomogeneous wave equation is inverted. The second term describes the acoustic source. In this way, a correspondence is established between the far sound field and the turbulent emission field.

The complete procedure was already described elsewhere [1, 2, 23]. In this paper we will give new results regarding 2.1 and 2.2 after a brief summary of this procedure and previous essential conclusions.

3. DESCRIPTION OF THE PROCEDURE

3.1. Measurement method

Since we are dealing essentially with hot jets (with expansion ratios between 1.2 and 3.4 and temperatures between 700° K and 1100° K) produced by propane combustion (anechoid chamber at the engine test center, Figure 1) or from kerosene combustion (ONERA Test Laboratory, Figure 2), the adapted method, inspired by Schetter [17], consists of collecting a small volume of the turbulent medium being studied with a receiver. The receiver is equipped with an appropriate infrared radiation optical device. The installation is shown in Figure 3.

Two receivers [24] with perpendicular axes and which are orthogonal with respect to the jet axis are utilized. Each of these receivers simultaneously analyzes the infrared emissions from all the points of the jet located in the vicinity of the optical axis. In the meantime, it has become possible to assign a certain spatial definition to these radiometers along this axis by installing a diaphragm along the optical path which has the function of a pupil. This means that the infrared emissions from the volume located at the position which is conjugate to the position of the diaphragm is given an increased weight. If the spatial definition is to be improved even more, it is necessary to use two instruments and their optical axes must cross at the point being studied. Also it is necessary to use a correlation method. /6.3

This configuration makes it possible to define the autocorrelation coefficient $\bar{C}(\vec{y}, o, \tau)$ of the infrared emission at the point under consideration. Finally, if the two axes are separated by a distance $\vec{y}$, the cross correlation coefficient $\bar{C}(\vec{y}, \vec{y}, \tau)$ is measured by plotting curves of C as a function

of τ for various values ξ, and the space-time turbulence parameters can be derived.

This type of measurement means that a refined mechanical installation will have to be available for displacing at least one of the radiometer optical axes in a precise way during the acoustic experiment.

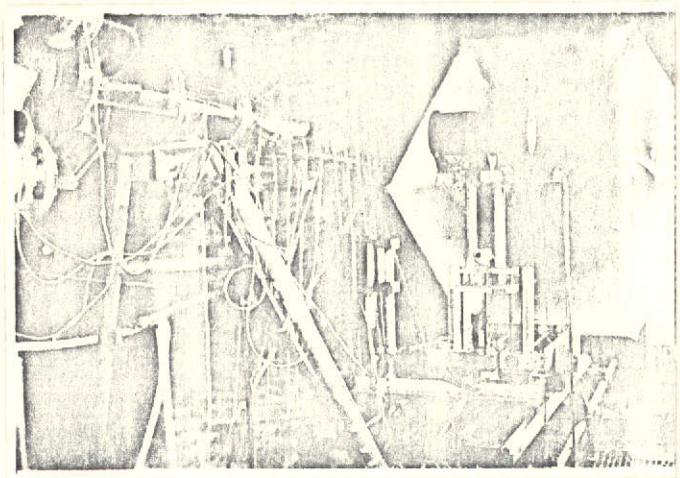

Figure 1. CEPr echo chamber.

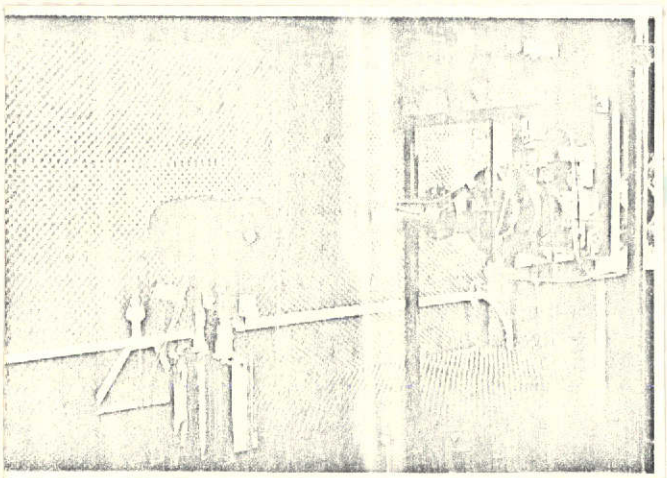

Figure 2. ONERA test cell.

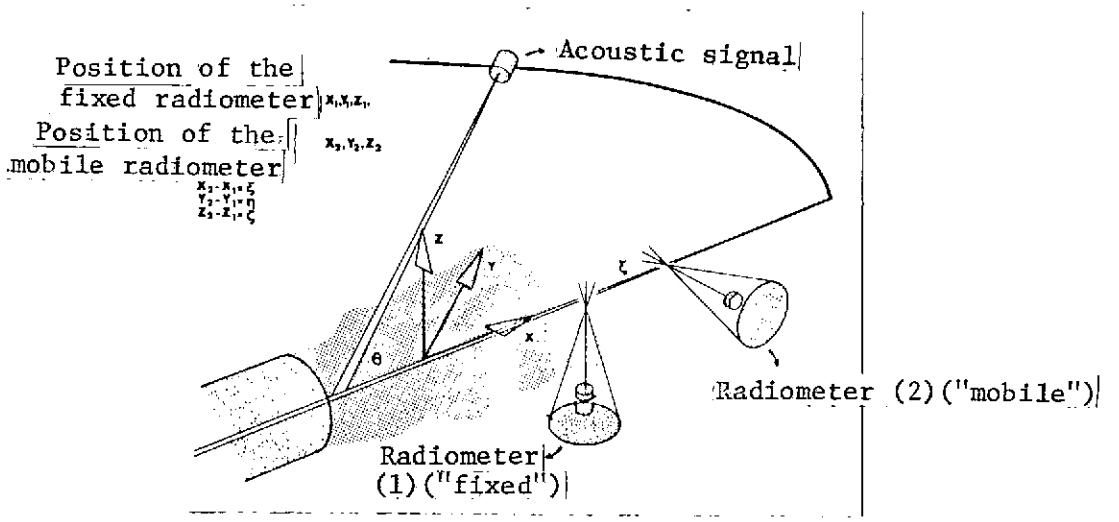

Figure 3. Principle of the installation

3.2. Hybrid signal processing.

3.2.1. Turbulence intensity

A radiometer located at various distances from the exit plane of the nozzle is displaced in the transverse direction. Each of the two radiometer measurement tracks provide the mean and root square $(\langle e^2 \rangle)^{1/2}$ and the average value $\langle E \rangle$ of the signal. The variation of the ratio $(\langle e^2 \rangle)^{1/2}/\langle E \rangle$ is a reflection of the mixing zone geometry. This ratio is related to the turbulence intensity and is a maximum at the end of the potential cone, which demonstrates the importance of this zone for the acoustic emission.

3.2.2. Space-time variables

Correlation coefficients $C_{11}(\xi, \tau)$ calculated from measurements are used to find characteristic turbulence variables using elementary calculations. The subscript 1 refers to

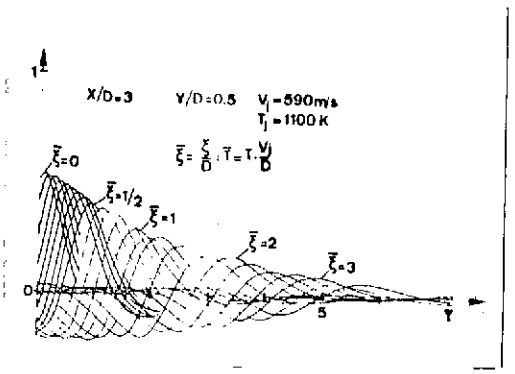

Figure 4. Variation of the correlation coefficients $c_{12}(\xi,\tau)$ for various axial differences $\varphi=\xi/D$ between the 2 radiometers.

Figure 5. Definition of a unique form of $c_{12}(\xi,\tau)$ using a double affinity.

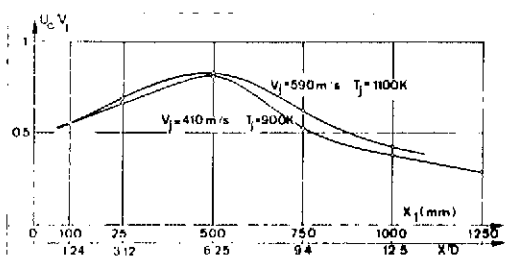

Figure 6. Axial profile of the convection velocity.

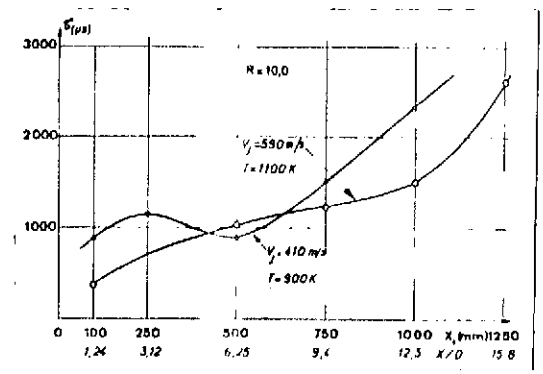

Figure 7. Axial profile of the integral scale of the lifetime.

radiometer 1, subscript 2 to the radiometer 2. ξ is equal to the separation between the axes which contain radiometers 1 and 2 (Figure 3) and τ is the delay.

Figure 4 shows an example of a correlation coefficient $C_{12}(\xi,\tau)$ calculated from measurements made in a zone N defined by the position of radiometer 1, the reference radiometer for the fixed radiometer. A first analysis of these correlations [25] shows that with a double affinity, the curves shown in Figure 4 can be superimposed (Figure 5). For any given X/D and for a given 2Y/D, it can be seen that most of the curve remains intact when ξ increases. Thus we can define a representative form of the correlation function in the zone under consideration. /6.4 This property also exists for measurements carried out at different positions X/D and 2Y/D within the jet.

Finally, it should be stated that any statistical study of a zone in the jet implies the hypothesis of a steady turbulent field. Mechanisms at an even larger scale could exist. Their contributions to the sonic radiation should also be studied.

In Figure 6 we give an example of the convection rate $V_c = \xi/\tau_M$ where τ_M is the abscissa of the maximum of the curve $C_{12}(\xi,\tau)$. It can be seen that this velocity passes through a maximum in the vicinity of the end of the potential cone.

Figure 7 shows an example of the axial profile of the integral scale of the lifetime $\theta = \int_0^\infty \bar{C}_{12}(\xi,\tau_M)\,d\xi$, where $\zeta_{12}(\xi,\tau_M)$ is the ordinate of the maximum of $\bar{C}_{12}(\xi,\tau)$.

Figure 8 gives an example of the actual profile on an integral scale of the axial correlation length $\mathcal{L}_x = \int_0^\infty C_{12}(\xi,0)\,d\xi$

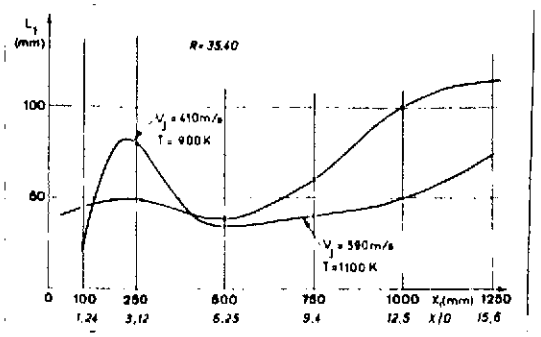

Figure 8. Axial profile of the integral scale of the axial correlation length.

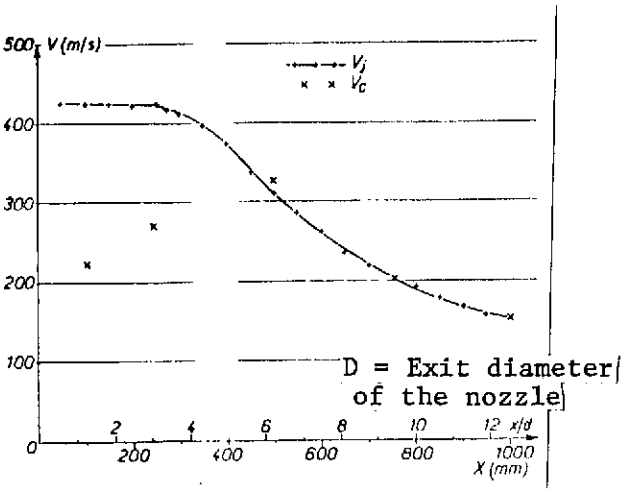

Figure 9. Velocity along the jet axis.

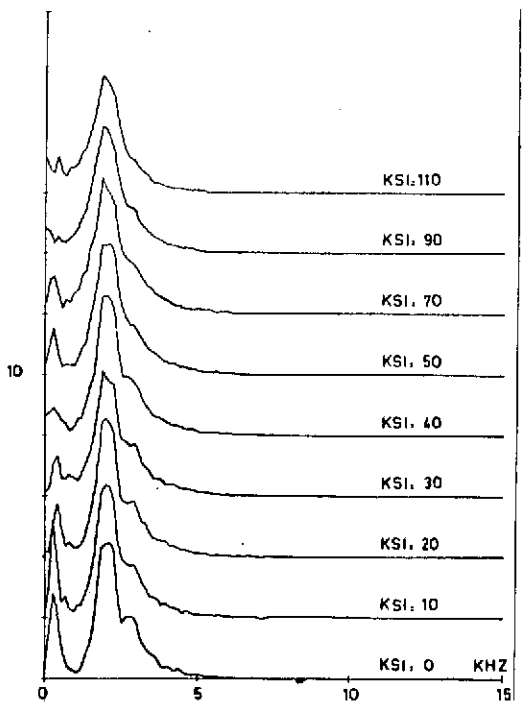

Figure 10. Infrared-infrared correlation.

where $C_{12}(\xi,0)$ is the ordinate of $C_{12}(\xi,\tau)$ at $\tau=0$.

3.2.3. Calculation of the acoustic field

Let us recall the major points of the calculation [23]:

from the wave propogation equation

$$\frac{\partial^2 \rho}{\partial t^2} - c_0^2 \Delta \rho = \vec{\nabla}\vec{\nabla}\vec{T}$$

/6.5

where ρ is the volume mass and

$$\vec{\vec{T}} = \rho \vec{v}\vec{v} - \vec{\vec{\varepsilon}} + (p - c_0^2 \rho)\vec{\vec{\pi}}$$

with $\vec{v}$ fluid velocity, p: pressure, c_0: acoustic velocity in the medium at rest and (*) the unit tensor. We derive:

$$p(\vec{x},t) = \sum_{i,j} \frac{x_i x_j}{4\pi c_0^2 x^2} \int_{V(\vec{y})} \left[\frac{\partial^2 T_{ij}}{\partial t^2}\right]_{\hat{t}} d\vec{y} \qquad (1)$$

where $p(\vec{x},t)$ is the acoustic pressure at $\vec{x}$ at the time t and $\hat{t} = t - \frac{|\vec{x}-\vec{y}|}{c_0}$, and $\vec{y}$ is a moving point in the volume source.

We can derive a complete formal description of the acoustic field using the following relationships:

3.2.3.1. Autocorrelation $P(\vec{x},\tau)$ of the far sound field

$$P(\vec{x},\tau) = \langle p(\vec{x},t)\, p(\vec{x}, t+\tau)\rangle$$

---

* Translator's note: Symbol omitted in foreign text.

$$P(\vec{x},t) = \frac{1}{16\pi^2 c_0^4 x^2} \int_{V(\vec{y})} d\vec{y} \int_{V(\vec{\eta})} d\vec{\eta} \left[\frac{\partial^4}{\partial \tau^4} \left\{ R_{\vec{x}}(\tau, \vec{y}, \vec{\eta}) \right\} \right]_{\tau = t + \tau''} \qquad (2)$$

with $\tau'' = \hat{t}'' - \hat{t}'$; $\vec{\eta} = \vec{y}'' - \vec{y}'$; $\vec{y} = \frac{1}{2}(\vec{y}' + \vec{y}'')$

($\vec{y}'$ and $\vec{y}''$ are two moving points of the volume source

and $R_{\vec{x}}(\tau, \vec{y}, \vec{\eta}) = \left\langle \frac{x_i x_j}{x^2} T_{ij}(\vec{y}, \hat{t}') \cdot \frac{x_k x_l}{x^2} T_{kl}(\vec{y}'', \hat{t}'' + \tau) \right\rangle$

3.2.3.2. Spectral density $I(\vec{x}, \omega)$:

$$I(\vec{x}, \omega) = \frac{2}{\pi \rho_0 c_0} \int_0^\infty P(\vec{x}, \tau) \cos \omega \tau \, d\tau \qquad (3)$$

3.2.3.3. Acoustic intensity $I(\vec{x})$:

$$I(\vec{x}) = \frac{\langle p^2(\vec{x}, t) \rangle}{\rho_0 c_0} = \frac{P(\vec{x}, 0)}{\rho_0 c_0} = \frac{\int I(\vec{x}, \omega) \, d\omega}{\rho_0 c_0} \qquad (4)$$

3.3 Essential conclusions from the first experiments:

The quantitative determination of the acoustic emissions with infrared emission measurements is not possible at the present time, because the signals cannot be controlled to scale. The first comparisons of the calculation results with acoustic

measurements and for two different operating ranges can only be of a quantitative nature.

These first comparisons showed that:

- the calculation gives the variations of the acoustic variables very correctly and, in particular, determines the following parameters:

  - the maximum emission angle,
  - the frequency of the maximum of the spectral density curve, for the maximum emission angle,
  - deviation between the maximum and minimum of the acoustic intensity.

In addition, the analysis of correlations [25] showed, as we pointed out in Section 3.2.2, that it is possible to give a representative form for the correlation function of the medium. This form differs considerably from the Gaussian form. These deviations cannot be explained by the limitations on the pass band of the instrumentation.

These latter observations led us to consider the turbulence model in order to represent the phenomena in a better way.

4. CHARACTERISTIC TURBULENCE VARIABLES

4.1. In Figure 6 we show an example of the axial profile of the convection rate. This rate is defined by the slope of the line $\zeta = f(z_M)$ where z_M is the abscissa of the maximum of the curve $c_{12}(\zeta, z)$ (Fig. 4).

Temperature and average pressure measurements in the free jet using a thermocouple and a Prandtl probe resulted in the velocity and average temperature profiles. We can therefore compare the convection rate derived from the correlations of the local velocity of the jet V_j. In Figure 9 we show an example of this comparison. In particular, we can observe that these two velocities coincide, up to the accuracy of measurement in the developed turbulence zone.

4.1.2. The various correlation coefficients $C_{12}(\bar{\xi}, \tau)$ were stored on a magnetic tape using a fast numerical Fourier transform program. The Fourier transform $C_{12}(\bar{\xi}, \omega)$ of the correlation coefficient is also calculated. From this we derive the cross spectral density (Figure 10) and the phase. From the phase we determine the convection rate for different frequencies, using an elementary calculation. Figure 11 a shows an example of the variation of the convection rate as a function of frequency.

In Figure 11b we show the curve $\bar{\xi} = f(\tau_M)$ derived from correlations. From this curve we can derive a convection rate which is representative of the entire spectrum. In Figure 11a we can see that it is quite similar to Figure 12 taken from reference [27]. In this particular case, the authors used a hot wire in a cold jet.

4.2. Length scale /6.7

From the correlations we derive (Figure 8) the integral scale of length which is representative for the entire spectrum.

The cross spectral density can be used to derive a length scale for each frequency of the spectrum for any point of the volume source.

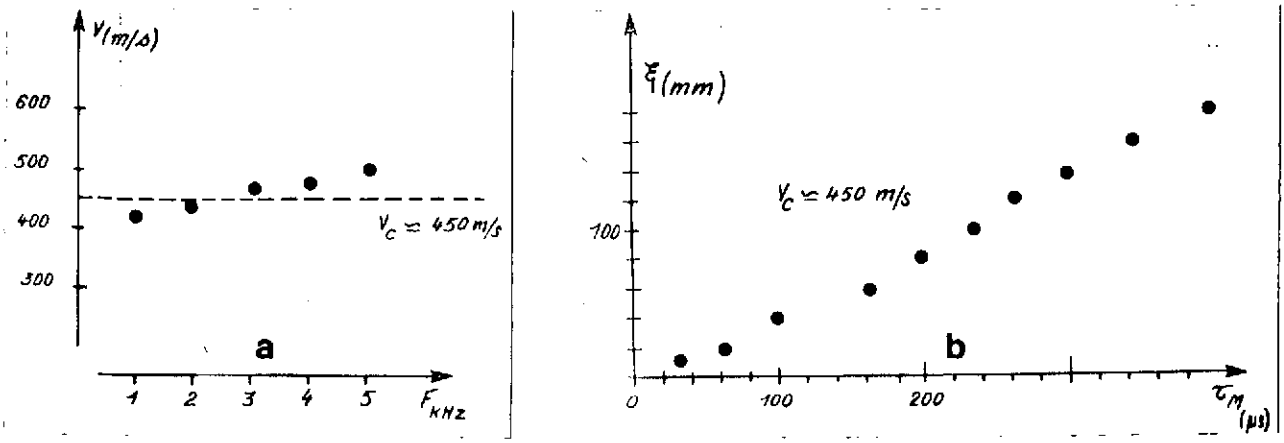

Velocity by frequency band Global convection rate

Figure 11. Convection rate

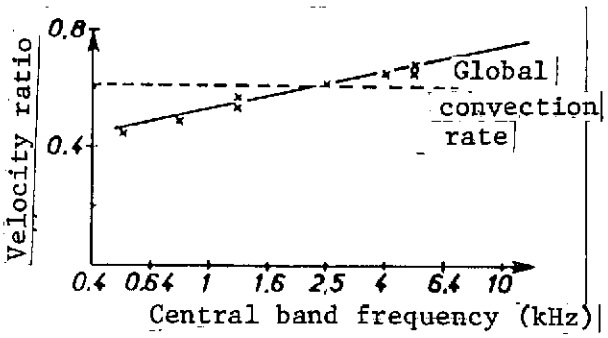

Figure 12. Variation of the convection rate by frequency band (Ref. [27]).

In Figure 13, we show the plot obtained after calculating the Fourier transforms, and these give the variation in the amplitude of the cross spectral density directly as a function of ξ (axial separation of the two radiometers). We can also derive the integral scale of length for the frequency under consideration. It can be seen that Figure 13 is similar to Figure 14, also taken from reference [27].

4.3. Consequences

This method of operation has two advantages:

4.3.1. The information is obtained rapidly and with a greater accuracy. Another method consisted of carrying out correlations with filtered signals. The number of correlations which must be calculated is equal to the number of selected frequencies. Because of filtering, the accuracy of the position of the maximum of the correlation coefficient is lost.

4.3.2. There is a better accuracy in the acoustical calculation of the sound field. The spectral densities and the phases (or convection rate for frequency bands) are known and therefore it is possible to replace the function $\mathcal{P}(\vec{x}, \tau)$ by $\mathcal{P}(\vec{x}, \omega)$ (or $I(\vec{x}, \omega)$) in the acoustic calculation (Section 3.2.3). This was simply taken into account by the assumed form of the spectrum and, on the other hand, the active region of each frequency band, which is then represented by the corresponding integral length scale, and not by a single integral scale for the entire spectrum.

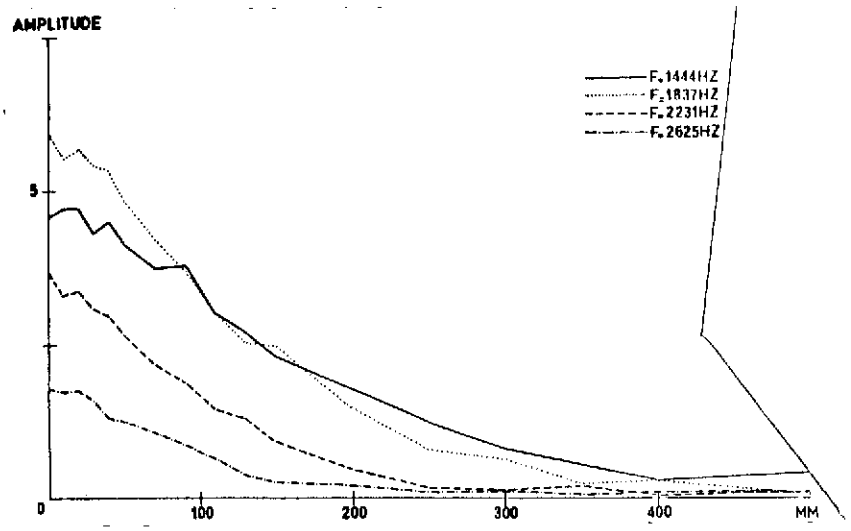

Figure 13. Length scale

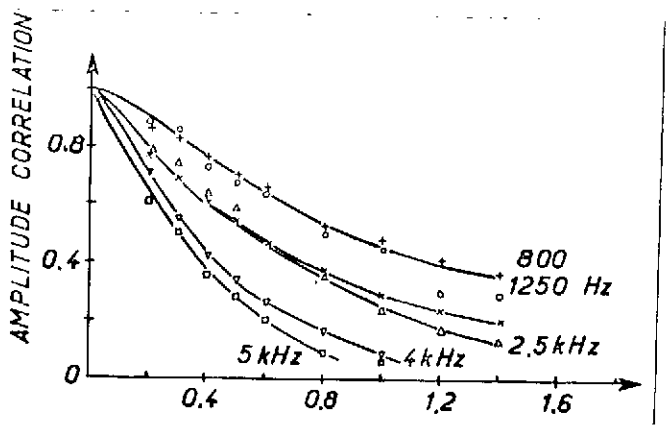

Figure 14. Rate of decrease of the maximum of correlation for various frequencies (ref [27]).

5. PHYSICAL INTERPRETATION OF THE INFRARED SIGNAL

The signal provided by the detectors and connected with the infrared emission of the warm jet is a function of concentration and temperature.

Laboratory measurements presently in progress will determine the law of variation of the signal as a function of these variables. Nevertheless, from the infrared sound correlation different kinds of information may be derived and we can therefore give a physical interpretation of the signal. In order to do this, microphones are placed in the near field, along a line parallel to the jet / 6.8 axis and at a distance sufficiently small so that each microphone will cover the acoustic radiation of one single section of the jet.

5.1. The spectral analysis of the microphone signal shows that the spectrum maximum decreases in a monotonic fashion when we move away from the nozzle outlet plane.

5.2. The spectral analysis of the infrared signal shows the same characteristics, but with a different slope.

5.3. The frequency and directivity of the contribution of the volume source observed with infrared in the sonic radiation is derived from the cross spectral densities. We will present a typical example:

- during measurements carried out in a free supercritical jet from a nozzle with a central body having a mechanical, structural silencer, the infrared-infrared correlation (Figure 15) shows that there is a spectral emission which is very pronounced around 13 KHz within a volume which has an axial limit of

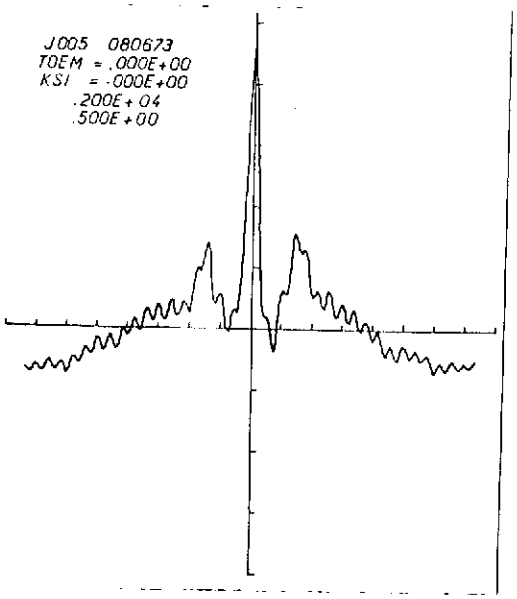

Figure 15. IR-IR correlation coefficient.

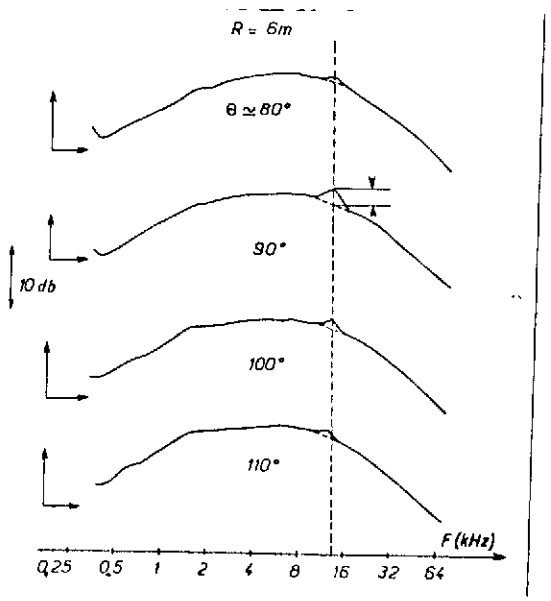

Figure 16. Spectrum (1/3 octave) as a function of θ .

about 140 mm (the nozzle diameter is about 90 mm).

From infrared-microphone correlations, with the microphone in the near field (at the radial distance of 400 mm), we were able to show that this particular spectral emission corresponds to an acoustic emission located in the same frequency band with a maximum radiation of about 90°.

These observations were performed at the ONERA installation where acoustic measurements in the far field are not very significant. These measurements were confirmed by other acoustic measurements in the echo chamber at the CEP_r - SACLAY at a radial distance of 6 m (acoustic measurements in the far field).

In Figure 16 we show the 1/3 octave spectral analyses of the microphone signal obtained in the far field for various angular positions θ (angle between the axis of the jet and the observation direction).

We can see that this emission is essentially a maximum for $\theta \simeq 90°$. Thus we were able to predict the acoustic consequences of a turbulent configuration located in a well-defined volume within the free jet. The analysis of such results using a frequency band is presently in progress [28].

REFERENCES

6.9

1. Taillet, J. Description and Establishment of a Method of Characterizing Noise Sources in Jets. 8th ICAS Congress, Amsterdam, 1972, ICAS Paper No. 72-35. L'Astr. and l'Astron. (1973-2) Translation NASA TT-F 14,851 (1973).

2. Richter, G. Study of Noise Sources of Cold Jets; being Published in the Periodical ENTROPIE.

3. Lighthill, R. J. Sound Generated Aerodynamically. The Bakerian Lecture, 1961. Proc. Roy. Soc., A, Vol. 267, 1962, p. 147.

4. Ribner, H. S. The Generation of Sound by Turbulent Jets. In "Advances in Applied Mechanics", Acad. Press, Inc., New York, Vol. 8, 1964.

5. FFOWCS-WILLIAMS, J. E. The Noise from Turbulent Convected at High Speed. Phil. Trans. Roy. Soc. Lond., A, Vol. 255, 1963, p. 469.

6. Kobrynski, M. General Method of Calculating the Sound Field Produced by Jet Aircraft Jets. Technical Note ONERA No. 187, 1971.

7. Potter, R. C. and J. H. Jones. An Experiment to Locate the Acoustic Source in High Speed Jet Exhaust Stream. 74th Meeting of the Acous. Soc. of America, Miami Beach, Florida, Nov. 1967.

8. Maestrello, L. Radiation from and Panel Response to a Supersonic Turbulent Boundary Layer. Boeing Report DI-82-0719, Sept. 1968.

9. Davies, P.O.A.L., M. J. Fisher and M. J. Barratt. The Characteristics of the Turbulence in the Mixing Region of a Round Jet. J. Fluid Mech., Vol. 15, 1963, p. 337.

10. Chu, W. T. Turbulence Measurements Relevant to Jet Noise. UTIAS Report No. 119, University of Toronto, 1966.

11. Siddon, T. E. and R. Rackl. Cross Correlation Analysis of Flow Noise with Fluid Dilatation as Source Fluctuation. Acoust. Soc. America, Fall. Meeting, 82nd Denver, Colo., Oct. 19-22, 1971, Paper tt. 12, 18 pages.

12. Davies, M. R. Quantitative Schlieren Measurements in a Supersonic Turbulent Jet. J. Fluid Mech., Vol. 51, 1972, p. 435.

13. Fisher, M. J. and N. Harper-Bourne. Private communication.

14. Wilson, L. N., F. R. Krause and K. A. Kadrmas. Optical Measurements of Sound Source Intensities in Jets. Basic Aerodynamic Noise Research - NASA SP-207, 1969, p. 147.

15. Fisher, M. J. and F. R. Krause. The Crossed Beam Correlation Technique. J. Fluid Mech., Vol. 28, 1967, p. 705.

16. Draper, J. S. Infrared Radiometry of Turbulent Flows. AIAA J., Vol. 4, 1966, p. 1597.

17. Schetter, K. A. Optical and Acoustical Measurements on Exhaust Plumes. EUROMECH 10, Liblice/Prague, 1968.

18. Dyer, I. Distribution of Sound Sources in a Jet Stream. J. Acoust. Soc. America, Vol. 31, 1959, p. 7.

19. Lee, H. K. Correlation of Noise and Flow of a Jet. UTIAS Report No. 168, University of Toronto, 1971.

20. Hoch, R. G., J. P. Duponchel, B. J. Cocking and W. D. Bryce. Study of the Influence of the Volume Mass of a Jet on its Acoustic Emission. First International Symposium on the Progress in Aircraft Jet Engines, Marseille, June, 1972.

21. Boa-Teh Chu and S. G. Leslie Kovasznay. Non-Linear Interaction in a Viscous Heat Conducting Compressible Gas. J. Fluid Mech. Vol. 3, Part 5, 1958.

22. The Lookheed-Georgia Company. The Generation and Radiation of Supersonic Jet Noise. Tech. report AFAPL-TR-72-53, July, 1972.

23. de Belleval, J. F., M. Perulli and G. Gauffre. Computation of the Sound Field of a Jet from Characteristic Turbulence Parameters Measured by Crossed-Beam Techniques. Opto-Electronics, Vol. 5, 1973.

24. Gauffre, G. and L. Gramont. Radiometers for Infrared Sounding of Free Jets. Nouvelle Revue d'Optique Appliquée, Vol. 3, No. 5, 1972, p. 267.

25. de Belleval, J. F. and M. Perulli. Measurement of the Correlation Function which Characterizes the Turbulence of a Free Jet. C. R. Ac. Sc. Paris, Vol. 274 A, 1972, pp. 1952-55.

26. de Belleval, J. F., M. Perulli, G. Richter and C. Schmidt. Preliminary Results of a Study of Infrared Emission from a Hot Jet. La Recherche Aérospatiale No. 1972-1, pp. 37-45.

27. Fisher, M. J. and P.O.A.L. Davies. Correlation-Measurements in a Non-Frozen Pattern of Turbulence. J. Fluid Mech. Vol. 18, 1964, p. 97.

28. de Belleval, J. F. Thesis, University of Paris, to be published.

Translated for National Aeronautics and Space Administration under contract No. NASw 2483, by SCITRAN, P. O. Box 5456, Santa Barbara, California, 93108.

STANDARD TITLE PAGE

1. Report No.	2. Government Accession No.	3. Recipient's Catalog No.
NASA TT F-15,233		

4. Title and Subtitle	5. Report Date
REPRESENTATION OF HOT JET TURBULENCE BY MEANS OF ITS INFRARED EMISSION	December, 1973
	6. Performing Organization Code

7. Author(s)	8. Performing Organization Report No.
Jean-François de Belleval and Mariano Pérulli	
	10. Work Unit No.

9. Performing Organization Name and Address	11. Contract or Grant No.
SCITRAN Box 5456 Santa Barbara, CA 93108	NASw-2483
	13. Type of Report and Period Covered
	Translation
12. Sponsoring Agency Name and Address National Aeronautics and Space Administration Washington, D.C. 20546	14. Sponsoring Agency Code

15. Supplementary Notes

Translation of: Représentation de la Turbulence D'un Jet Chaud A Partir de Son Emission Infrarouge. Office National d'Etudes et de Recherches Aérospatiales, 92320 Chatillon, France, September 17-21, 1973 Report T.P. No. 1277, 10 pages.

16. Abstract

The theoretical description of a jet acoustic radiation is usually described by characteristic turbulence data, defined at the scale of the total emissive volume. These data are deduced from theoretical models of from measurements making use of correlation techniques. Hence these data have average values in time, i.e. representing the whole spectrum.

In this paper, after a discussion on the nature of acoustic sources which may exist in a hot jet, and after recalling the crossed beam techniques, is presented, on examples, a representation of a hot jet turbulence by means of crossed spectral densities. It is then possible to define at any point of the source volume the characteristic turbulence data by frequency bands, and thus to know their dispersion.

17. Key Words (Selected by Author(s))	18. Distribution Statement
	Unclassified - Unlimited

19. Security Classif. (of this report)	20. Security Classif. (of this page)	21. No. of Pages	22. Price
Unclassified	Unclassified	23	